Experimental levitation of dust grains in a plasma sheath

A. A. Sickafoose and J. E. Colwell
Laboratory for Atmospheric and Space Physics, University of Colorado, Boulder, Colorado, USA

M. Horányi and S. Robertson
Department of Physics, University of Colorado, Boulder, Colorado, USA

Received 23 February 2002; revised 8 May 2002; accepted 10 June 2002; published 27 November 2002.

[1] Dust grains have been observed to levitate above the surface of the Moon and as spokes in Saturn's rings. In order to gain a better understanding of these observations, we have performed levitation experiments on dust grains in a low-density plasma. Plasma sheath potential profiles, measured by an emissive probe, are used to determine the spatial dependence of the electric force on a grain in the sheath. The observed levitation height agrees with the values calculated using orbital-motion-limited charging theory and force balance equations. Levitating grains were also exposed to an ultraviolet light source to induce photoemission. Three types of dust were investigated: polystyrene divinylbenzene microspheres 10.0 ± 0.5 μm in diameter, glass microballoons <38 μm in diameter, and JSC-1 (lunar regolith simulant) <25 μm in diameter. Our experimental results show that (1) various types and sizes of grains can levitate in a plasma sheath above a conducting surface; (2) levitating grains of a standard size float at a height corresponding to that predicted by theory; (3) exposure to UV light causes the grain levitation height to decrease slightly as a result of less negative charge; and (4) a mechanism to inject grains into the sheath is not necessary if the electric field is sufficiently strong. *INDEX TERMS:* 7831 Space Plasma Physics: Laboratory studies; 7819 Space Plasma Physics: Experimental and mathematical techniques; 6213 Planetology: Solar System Objects: Dust; 6015 Planetology: Comets and Small Bodies: Dust; *KEYWORDS:* experimental, dust

Citation: Sickafoose, A. A., J. E. Colwell, M. Horányi, and S. Robertson, Experimental levitation of dust grains in a plasma sheath, *J. Geophys. Res.*, *107*(A11), 1408, doi:10.1029/2002JA009347, 2002.

1. Introduction

[2] Prime examples of active dust transport near surfaces of airless bodies in the solar system include dust grains suspended above the lunar surface observed by the Surveyor spacecraft and the Apollo missions, [e.g., *Singer and Walker*, 1962; *Rennilson and Criswell*, 1974; *Pelizzari and Criswell*, 1978; *Zook and McCoy*, 1991], more recent images of scattered light along the lunar limb by the Clementine spacecraft [*Zook et al.*, 1995], spokes observed in Saturn's rings [*Goertz*, 1989; *Nitter et al.*, 1998], and newly acquired images of dust-filled craters from the NEAR spacecraft at Eros [e.g., *Veverka et al.*, 2001; *Robinson et al.*, 2001]. Electrostatic dust levitation and transport have been theorized to occur on Mercury [*Ip*, 1986], asteroids [*Lee*, 1996], and comets [*Mendis et al.*, 1981]. Since dusty regoliths are produced by the interplanetary micrometeoroid flux on nearly all airless bodies in the solar system, understanding dust charging and dynamics above surfaces is important for interpreting remote sensing data and analyzing the evolution of these planetary surfaces.

0148-0227/02/2002JA009347$09.00

[3] Objects in a plasma, such as planetary bodies in the solar wind, charge to a floating potential determined by the balance between charging currents in the local plasma environment. The primary charging currents are due to collection of electrons and ions from the plasma, photoemission, and secondary electron emission. In cases where secondary electron emission and photoemission are weak, objects will become negatively charged due to electron collection and will be surrounded by a plasma sheath (unless the ion temperature is much greater than the electron temperature). Negatively charged dust grains from these surfaces can thus be levitated in a plasma sheath above the surface at a height where the gravitational force is balanced by the electric force, or can be accelerated to the escape velocity. This interaction between charged dust grains and plasma sheaths above surfaces is one proposed mechanism for dust levitation and transport on airless bodies throughout the solar system. Photoelectron sheaths provide another mechanism for levitation and transport of dust near the terminator [e.g., *Criswell*, 1972; *Sickafoose et al.*, 2001].

[4] Experiments on the levitation of lunar regolith simulant in a strong electrical field with and without UV were performed by *Doe et al.* [1994]. Experiments demonstrating the levitation of hollow glass microballoons in a plasma sheath have been performed by *Arnas et al.* [1999, 2000,

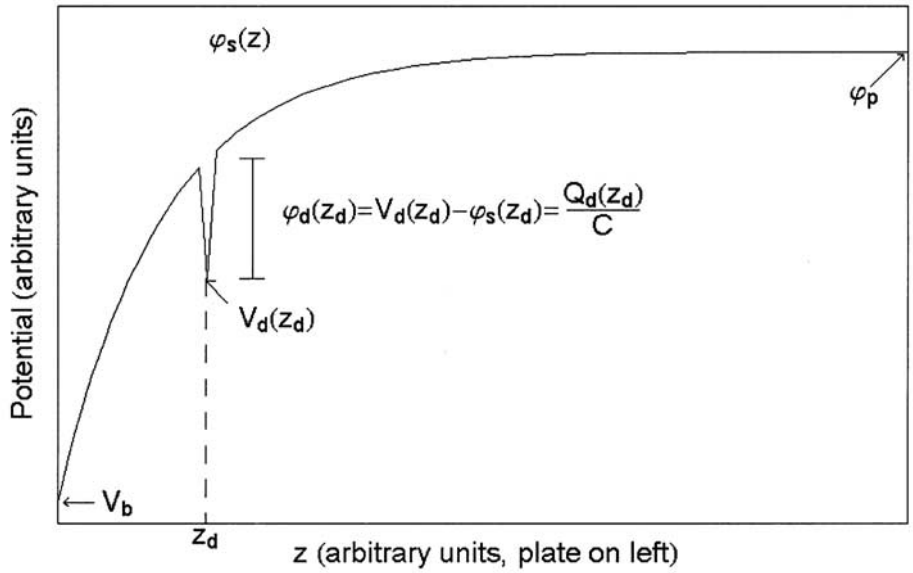

Figure 1. A schematic diagram of the local potential as a function of distance from a surface, $\varphi_s(z)$. The dip in the local potential represents a negatively charged dust grain embedded in the plasma sheath at distance z_d from the surface. The dust potential is labeled $V_d(z_d)$. In order to calculate the charge on the grain, the dust potential with respect to the local plasma potential is required, where $\varphi_d(z_d) = V_d(z_d) - \varphi_s(z_d) = Q_d(z_d)/C$. The plasma potential, φ_p, and surface potential, V_b, are also labeled.

2001]. *Sickafoose et al.* [2000, 2001] studied the charging of lunar regolith simulant in a photoelectric sheath above a surface, in order to gain an understanding of grain charging on planetary surfaces exposed to UV light and lacking an atmosphere or magnetic field. In the presence of an atmosphere, the charging processes would be greatly modified. The present work consists of experiments on the charging and levitation of grains with a careful comparison to models applicable for planetary surfaces.

[5] We have conducted experiments on the levitation of dust grains in an argon plasma sheath above a horizontal conducting surface. The purpose of these experiments is not to simulate the conditions found in the solar system, but to create situations in which the applicable model equations can be verified. We create conditions in laboratory plasma in which dust grains are levitated above a surface and show that the data are consistent with a theoretical model. Types of levitated dust particles include polystyrene microspheres of an accurately known size, glass microballoons, and JSC-1, a lunar regolith simulant.

[6] We employ a combination of Langmuir and emissive probe measurements to fully characterize the plasma in the sheath (i.e., densities, temperature, plasma potential, and the electric field) and measure the height where dust grains are levitated. From the height measurement we determine the charge on the grain by two methods: (1) using orbit-motion-limited (OML) charging theory [*Bernstein and Rabinowitz*, 1959] with the appropriate plasma parameters at that height and (2) balancing the gravitational force and the electric force, using our electric field measurements as input. In the latter case, we also show that grains levitate at a stable equilibrium point. The close agreement between the charges deduced from these two methods indicates that we correctly characterized our sheath and the charging processes. Hence the details of this model can be applied to conditions elsewhere.

[7] In section 2, we present the charging currents and the forces on a dust particle within the sheath. In section 3, we describe the experimental apparatus and the measurements. We find the grain potential and charge by the two methods mentioned in the previous paragraph. Then, we compare the observed levitation heights with the stable levitation heights calculated from OML theory and force balance equations. The effects of exposure to UV light on a levitated particle are also discussed. In section 4, conclusions and future work are presented.

2. Dust Levitation Model

2.1. Charging Currents

[8] An expression for the charge on an isolated dust grain in a low temperature laboratory plasma is usually obtained using "orbit motion limited" theory [*Bernstein and Rabinowitz*, 1959]. This theory considers the grains to be spherical probes with grain radius much less than the electron Debye length, $r_d \ll \lambda_d$. The charge on a grain is related to the dust potential at any location z above the surface by

$$Q_d(z) = C\varphi_d(z) = 4\pi\varepsilon_0 r_d(V_d(z) - \varphi_s(z)), \qquad (1)$$

where $C = 4\pi\varepsilon_0 r_d$ is the capacitance of a spherical grain with radius r_d. The dust potential, $\varphi_d(z) = V_d(z) - \varphi_s(z)$, is the difference between the dust potential relative to ground, $V_d(z)$, and the local plasma potential, $\varphi_s(z)$. For clarity, Figure 1 shows a schematic diagram of a negatively charged dust grain embedded in a plasma sheath with each of these potential values labeled. Also labeled in Figure 1 are the

plasma potential, φ_p, and the potential, V_b, of the surface beneath the sheath.

[9] Charging currents to the grain in a collisionless plasma are calculated by assuming the dust grain collects electrons and ions if their orbits intersect the grain. This calculation often includes a contribution from the primary, energetic electrons used to create the plasma [*Walch et al.*, 1995]. In our experiment, the ionization filament is located below the surface; therefore the dust grains are not charged by any primary electrons. The resulting equilibrium charge of a grain in the sheath is that at which the electron current, $I_e(z)$, and the ion current, $I_i(z)$, balance:

$$I_e(z) + I_i(z) = 0. \tag{2}$$

[10] In order to calculate the charging currents, the ion and electron densities within the sheath are required. Assuming the plasma electrons have a velocity distribution that is approximately Maxwellian, with temperature T_e, the electron density follows the Boltzmann relation:

$$n_e(z) = n_0\, Exp\left[\frac{e\left(\varphi_s(z) - \varphi_p\right)}{kT_e}\right], \tag{3}$$

where n_0 is the density in the bulk plasma, e is the elementary charge, and φ_p is the plasma potential.

[11] Ions are assumed to be cold in the bulk of the plasma, and they are accelerated into the sheath by the potential gradient. In the Bohm model, the region in between the (nonneutral) sheath and the (neutral) plasma, called the presheath, is assumed to accelerate the ions to the sound speed, $c_s = \sqrt{kT_e/M}$, where M is the ion mass [e.g., *Bohm*, 1949; *Lieberman and Lichtenberg*, 1994]. This assumption is necessary because the equations for the sheath have solutions only when the ion velocity, $v_i(z)$, is greater than or equal to c_s. Using conservation of energy, the ion velocity within the sheath can then be written as

$$v_i(z) = \sqrt{c_s^2 - \frac{2e(\varphi_s(z) - \varphi_0)}{M}}, \tag{4}$$

where φ_0 is the plasma potential at the sheath boundary.

[12] At the sheath-presheath boundary, the ions entering into the sheath are accelerated to the Bohm velocity when the potential drop is 1/2 kT_e. Thus the potential at the sheath edge is $\varphi_0 = \varphi_p - 1/2\ kT_e$. At this position, the electron and ion densities are related to the density in the plasma by

$$n_{i,e} = \exp\left[\frac{-e\left(\varphi_p - \varphi_0\right)}{kT_e}\right] n_0 = \exp\left(\frac{-1}{2}\right) n_0 \approx 0.16 n_0. \tag{5}$$

[13] The continuity equation is then used to write an expression for ion density in the sheath,

$$n_i(z) \approx 0.16 n_0 \left[1 - \frac{2e(\varphi_s(z) - \varphi_0)}{Mc_s^2}\right]^{-1/2}. \tag{6}$$

[14] From equation (3), the current to a negatively charged grain from thermal electrons is

$$I_e(z) = -\frac{A}{4} e\, n_0 \sqrt{\frac{8kT_e}{\pi m_e}} \exp\left[\frac{e\left(V_d(z) - \varphi_p\right)}{kT_e}\right], \tag{7}$$

where A is the surface area of the grain ($A = 4\pi r_d^2$), and m_e is the electron mass. From equation (6), the corresponding ion current to a negatively charged grain is

$$I_i(z) = \frac{A}{4} e\ 0.61 n_0 c_s \left[1 - \frac{2e(V_d(z) - \varphi_s(z))}{M v_1(z)^2}\right]. \tag{8}$$

Equations (2), (7), and (8) are used with experimental values for T_e, n_0, $\varphi_s(z)$, and φ_p to solve for the dust grain potential with respect to the local plasma, $\varphi_d(z)$. For a given grain size and density, equation (1) then provides the dust charge $Q_d(z)$. Dust grain potentials and charges calculated using this model are referred to as $\varphi_{d\mathrm{OML}}(z)$ and $Q_{d\mathrm{OML}}(z)$.

2.2. Forces on a Dust Grain

[15] The forces on a dust grain in the sheath are neutral drag, ion drag, the electric force in the sheath, and gravity. Collisions with neutral gas atoms cause a drag force acting opposite to the direction of dust motion. The neutral gas pressure is <1 mtorr, and the dust grains are observed to be practically motionless; therefore this force can be ignored. The ion drag force is caused by momentum transfer from the positive ion current driven by the electric field and acts toward the surface. It has two components: direct collisions (transfer of momentum from all ions collected by the grain) and Coulomb collisions. The ion drag force, calculated following *Samsonov et al.* [2001], is on the order of 10^{-16} N. This is a factor of 10^4 less than the gravitational and electric forces, so the ion drag force is also negligible. The two primary forces on a grain in the sheath are the electric force, $F_e(z)$ (acting away from the surface), and gravity, F_g (acting toward the surface). A grain is levitated when these forces balance and

$$F_e(z) - F_g = 0. \tag{9}$$

[16] The upward force on a spherical grain in the sheath due to the electric field perpendicular to the surface, $E(z)$, is

$$F_e(z) = Q_d(z)E(z) = -4\pi\varepsilon_0 r_d \varphi_d(z) \frac{\partial \varphi_s(z)}{\partial z}. \tag{10}$$

The downward gravitational force on the grain is

$$F_g = m_d g = \frac{4}{3}\pi r_d^3\, \rho_d\, g, \tag{11}$$

where m_d is the mass of the grain, ρ_d is the grain density, and g is the acceleration due to gravity.

[17] In order to determine the stability of an equilibrium point, the total mechanical potential is calculated as

$$U(z) = -\int_0^z \left(F_e(z') - F_g\right) dz'. \tag{12}$$

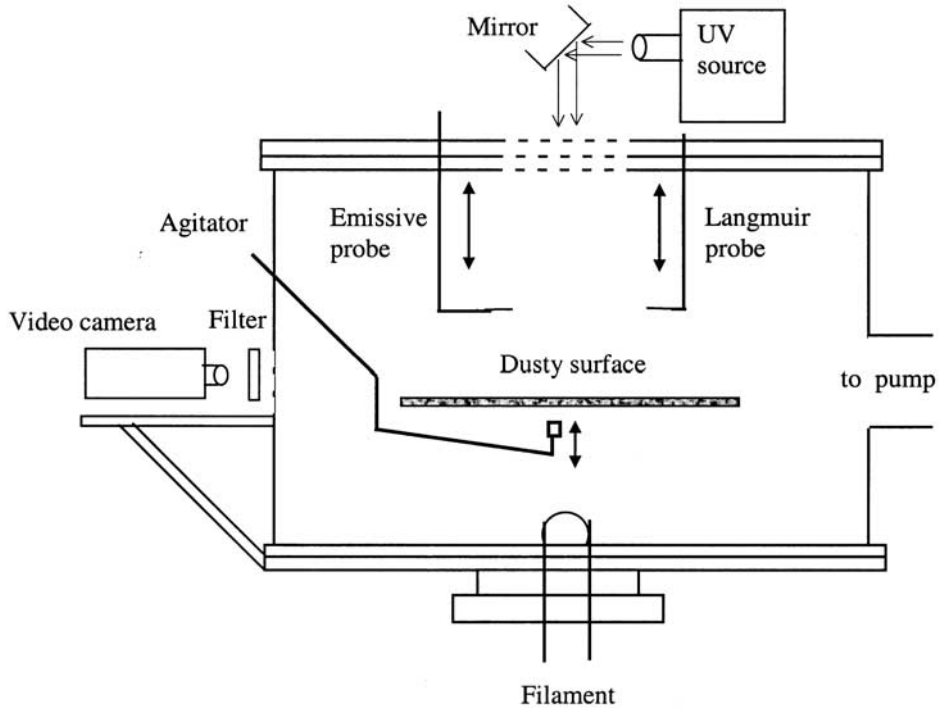

Figure 2. Schematic drawing of the chamber. A conducting surface rests in the center of the chamber, above which dust grains are levitated. A laser sheet (not shown in this drawing but shining out of the page) is directed perpendicular to the video camera to allow viewing of dust grains.

Stable equilibrium points are minima in the potential while unstable equilibrium points are maxima. Given the particle size and density, and the emissive probe data for $\varphi_s(z)$, equations (9), (10), and (11) are used to calculate $\varphi_d(z)$. Equation (1) then provides an experimental value for the dust charge $Q_d(z)$ which can be compared with the theoretical value calculated from equations (2) and (1).

3. Experimental Results

3.1. Apparatus, Materials, and Diagnostic Tools

[18] The experiments are conducted in a cylindrical stainless steel vacuum chamber 51 cm in diameter and 28 cm deep. The schematic diagram for the chamber is shown in Figure 2. The chamber is evacuated to approximately 2×10^{-7} torr by a turbomolecular pump. For experiments, the chamber is filled with argon gas to a pressure of 1.5×10^{-4} torr. The ionization source is a tungsten filament (0.025 mm diameter, $\sim$10 cm long) located underneath the surface. This filament is biased to -40 V and has a typical emission current of 350 mA, creating the primary electrons that ionize gas in the chamber. The resulting plasma is collisionless and is assumed to be Maxwellian. The filament position below the surface prevents charging of dust grains on the surface by primary electrons.

[19] Plasma characteristics are measured by a Langmuir probe and an emissive probe inside the chamber. The Langmuir probe is used to determine n_0, T_e, and φ_p. The emissive probe is used to measure the local potential as a function of position in the chamber [*Diebold et al.*, 1988]. These measurements provide the vertical potential profile in the sheath, $\varphi_s(z)$. The potential on the emissive probe at $z > 7$ cm corresponds to the plasma potential, φ_p. The Langmuir probe and emissive probe data concur on the value of the plasma potential.

[20] Dust grains rest on a horizontal, conducting surface $\sim$30 cm in diameter in the middle of the chamber. The electric field above the surface is controlled by connecting the surface to an external power source. The use of a conducting surface allows the surface potential to be varied so that its effect upon levitation height can be found and compared with the model. Also, the dark side of the lunar surface (and other planetary surfaces in the solar wind) and can reach large negative biases. We use a conducting surface in our laboratory setup to reach similar biases. An insulated hammer underneath the surface can be manually activated to agitate and inject dust into the sheath. Manual agitation is not always necessary. Grains have been observed to separate from the surface and achieve levitation when it is biased to < -30 V without agitation.

[21] In order to view dust grains on and above the surface, illumination is provided by an air-cooled argon laser. The laser beam passes through a cylindrical lens, producing either a horizontal laser sheet above the surface at a specific height or a vertical sheet. A viewing window perpendicular to the incoming laser sheet allows observation of the dust by a video camera. A narrowband filter (488 ± 2 nm) rests in front of the video camera. This allows the laser light reflected from dust grains to be observed while incident light from the filament and outside of the chamber is nearly eliminated. The UV source used in some experiments is a

Table 1. Properties of Dust Grains Levitated in the Experiments

Dust Type	Size Range of Diameter, μm	Density, (^{g}/cm^3)
Polystyrene DVB microspheres	10.0 ± 0.5	1.05
Hollow glass microballoons	<38	0.35
JSC-1	<25	2.9

1 kW Hg-Xe arc lamp, which is reflected off an $AlMgF_2$ mirror (80% reflective at 200 nm) and is incident at an angle normal to the surface.

[22] Three different types of dust grains are levitated in the experiments: polystyrene DVB (divinylbenzene) microspheres, hollow glass microballoons, and JSC-1 (lunar regolith simulant). The JSC-1 is used because its chemical composition and mineralogy fall within the ranges of lunar mare soil samples [*McKay et al.*, 1994]. The physical properties of the grains are listed in Table 1. All samples are obtained in granular form, and the glass and JSC-1 are dry sieved from a larger size distribution. The polystyrene microspheres were chosen because they have a narrow size distribution that allows calibration of the experiment through comparison with a theoretical model. The glass microballoons were chosen because they have a large charge-to-mass ratio and are thus more easily levitated. While the glass microballoons and polystyrene microspheres are spherical, JSC-1 grains are a variety of shapes [*Sickafoose et al.*, 2001].

3.2. Characterization of the Plasma Environment

[23] The Langmuir probe measurements indicate a background electron density of $n_0 = 2\ (\pm 1) \times 10^7$ cm^{-3}, electron temperature $T_e = 3.6\ (\pm 0.2)$ eV, and a plasma potential $\varphi_p \cong 1.7$ V. These parameters give an electron Debye length of $\lambda_d \cong 0.3$ cm. In order to determine the sheath potential profile above the surface, data from the emissive probe is taken from approximately 0.6 to 7.0 cm from the surface at 0.05 cm increments. The emissive probe circuit finds the potential at which electrons leave a heated filament, a value that differs negligibly from the local space potential [*Diebold et al.*, 1988]. Figure 3a shows the measured potential in the sheath as a function of distance from the surface. These data are taken for a range of surface biases: −80 V, −70 V, −60 V, −50 V, and −40 V. The potential profiles are well fit by the function

$$\varphi_s(z) = a - b\, e^{-cz}, \tag{13}$$

so that the electric field in the sheath is given by

$$E(z) = -\frac{\partial \varphi_s(z)}{\partial z} = -bc\, e^{-cz}, \tag{14}$$

where a corresponds to the plasma potential, b corresponds to the surface bias, and c is a free parameter [*Arnas et al.*, 1999, 2000, 2001].

[24] Under typical plasma conditions, the surface has a measured floating potential of $\varphi_f = -29$ V. When a sheath is driven to more negative voltage, in this case having a surface bias $V_b < \varphi_f$, the sheath height can be much larger than the Debye length. For the measured values of plasma potential and electron temperature, the

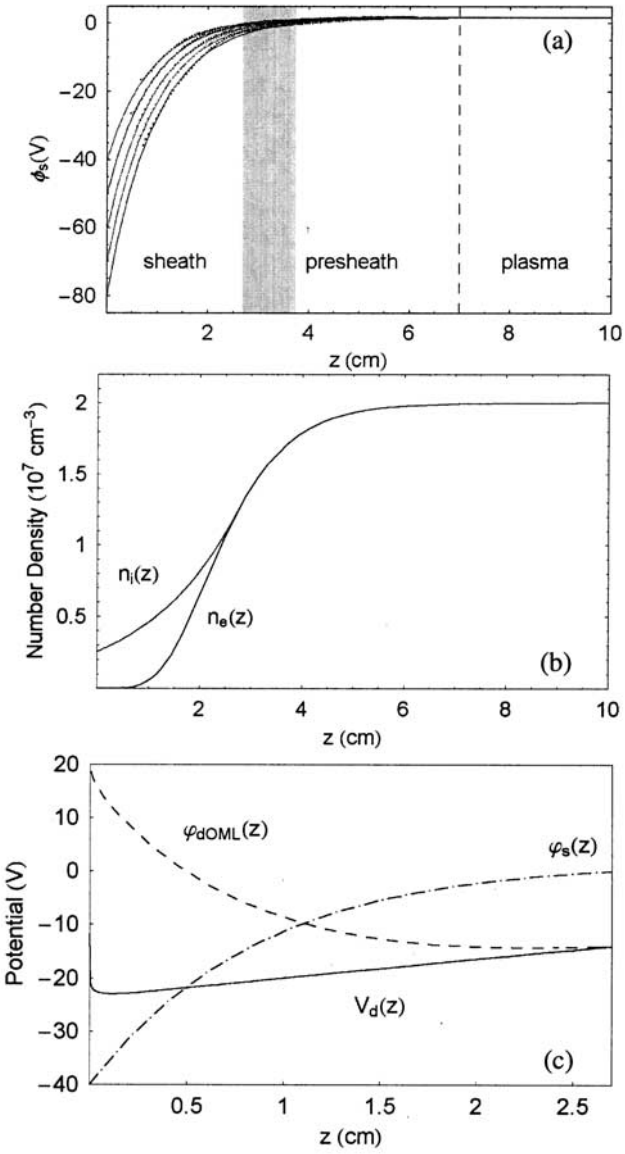

Figure 3. Plasma sheath characteristics. (a) Sheath potential profiles as a function of distance from the surface, $\varphi_s(z)$. The data points are measured by the emissive probe for five different surface biases: −40 V, −50 V, −60 V, −70 V, and −80 V. Solid lines are least squares fits to the data calculated from equation (13). Three general regions, the sheath, presheath, and bulk plasma are denoted. The shaded rectangle denotes the range of distances from the plate at which $\varphi_s = 0$ V for each surface bias. The inner edge of the rectangle corresponds to the sheath extent for $V_b = -40$ V, while the outer edge is the sheath extent for $V_b = -80$ V. (b) The electron and ion densities are found using equations (3) and (6), respectively, for a surface biased to −40 V. (c) The local sheath potential for a surface biased to −40 V is shown as a dot-dashed line, along with the model dust grain potential. The dust potential with respect to the local potential, $\varphi_{d\mathrm{OML}}(z)$ is calculated from equations (2), (7), and (8) and is the dashed line. The dust potential with respect to the bulk plasma, the solid line, is given by $V_d(z) = \varphi_{d\mathrm{OML}}(z) + \varphi_s(z)$. This plot extends to the sheath edge, because dust charging calculations are valid only within the sheath.

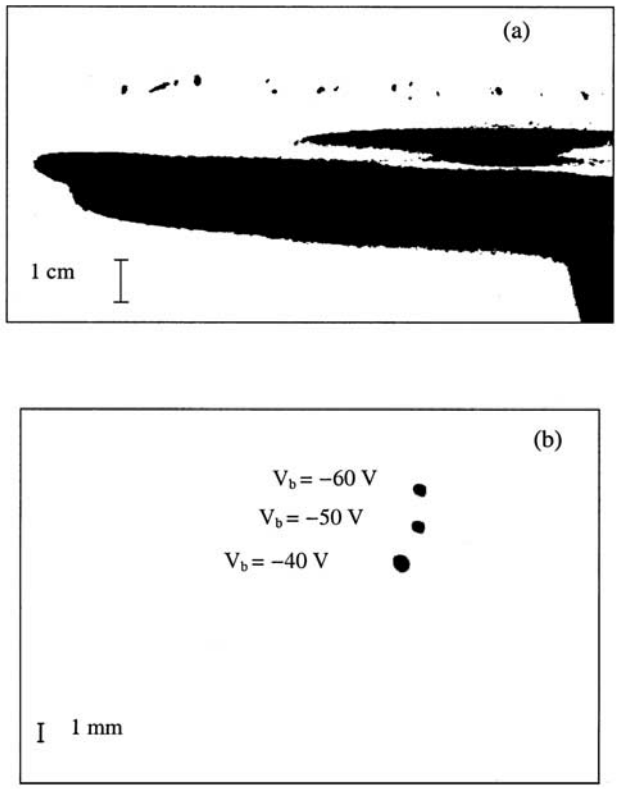

Figure 4. (a) Negative and schematic drawing of a digital photograph of levitating JSC-1 dust. There is a cloud of dust illuminated in the laser beam approximately 1.1 cm above the surface. (b) Negative of three superimposed digital photographs showing a stable, levitated polystyrene DVB grain (10.0 μm in diameter) for the surface at three different biases: −40V, −50 V, and −60 V. As expected, the grain is at the highest position away from the surface when the surface bias is most negative.

Bohm criterion $\varphi_p - \varphi_0 = 1/2\ kT_e = 1.7$ V is satisfied at $\varphi_0 = 0$ V. When $V_b = -40$ V this occurs at a distance from the surface of $z = 2.7$ cm. The measured sheath thickness is consistent with the Bohm model for a Debye length of 0.2 cm rather than the 0.3 cm indicated by analysis of the probe data. This discrepancy can be explained by the density from the probe measurement being too small. The density is deduced from the point of saturation of the probe current which is difficult to determine and leads to an uncertainty of a factor of a few. The temperature is determined from the slope of the current-voltage characteristic and can be determined more accurately than the density. However, the value of the density does not affect the calculation of the grain potential or charge. The electron and ion currents, equations (7) and (8), contain density as a multiplicative factor and thus the potential at which the currents balance is independent of density. Beyond the sheath, the presheath extends to a distance of roughly 7 cm from the surface at which point the plasma potential is typically reached.

[25] It is useful to have a visual representation of the sheath characteristics for the measured conditions. The sheath, presheath, and plasma regions are labeled in Figure 3a. Figure 3b shows the densities of ions and electrons with distance from the surface using equations (3) and (6). In Figure 3c, the local sheath potential is shown along with the OML dust potential calculated from equation (2) for a 10.0 μm polystyrene particle in the sheath. This plot demonstrates how a particle very close to the surface is charged positively due to the high density of ions, while a particle farther away from the surface will collect electrons and become negatively charged. The surface is assumed to be biased to −40 V for Figures 3b and 3c.

3.3. Dust Levitation Experiments

3.3.1. Levitation of Polystyrene Microspheres

[26] The glass microballoons and the JSC-1 dust span a large size range, so the precisely sized polystyrene microspheres are used to compare the particle potential as a function of surface bias to the potential predicted from the OML model. Digital photographs of levitating polystyrene and JSC-1 grains are shown in Figure 4. As the surface voltage is made more negative in the experiments, the levitation height of a 10.0 (±0.5) μm polystyrene grain increases (photograph in Figure 4b, data plot in Figure 5a). This is expected, since the electric field in the sheath increases for decreasing surface biases and the potential

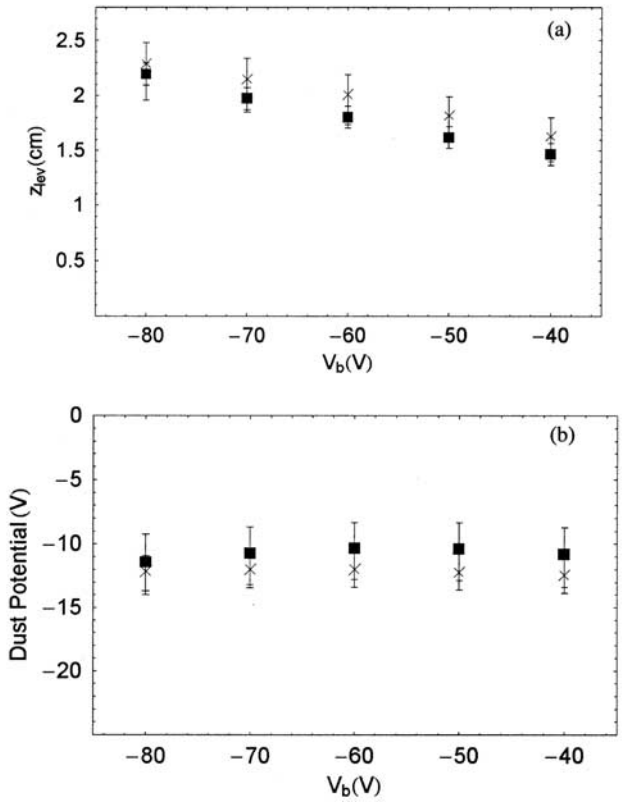

Figure 5. (a) Levitation heights, z_{lev}, and error bars for polystyrene grains as a function of surface bias. The boxes are experimental levitation heights, and the crosses are heights calculated by equating $\varphi_{d\mathrm{OML}}(z)$ to $\varphi_d(z)$ and selecting the stable equilibrium height. (b) The average potential on a levitating polystyrene grain at each surface bias from the theoretical model, $\varphi_{d\mathrm{OML}}$ (represented by crosses), and deduced from the experiments, φ_d (represented by boxes), given the observed levitation height.

Table 2. Experimental Data for Levitated Polystyrene Grains in the Plasma Sheath

Surface Bias, V_b, V	Measured Levitation Height, cm	Potential at Measured Height, φ_d, V	Charge at Measured Height, Q_d, (10^4 e)	Electric Field at Measured Height, E, V/cm
−80	2.20 ± 0.1	$-11.42 \pm \frac{2.19}{2.57}$	$-3.96 \pm \frac{0.76}{0.89}$	$-8.49 \pm \frac{0.85}{0.94}$
−70	1.98 ± 0.1	$-10.72 \pm \frac{2.04}{2.47}$	$-3.72 \pm \frac{0.71}{0.86}$	$-9.05 \pm \frac{0.94}{1.04}$
−60	1.80 ± 0.1	$-10.34 \pm \frac{1.98}{2.41}$	$-3.59 \pm \frac{0.69}{0.84}$	$-9.37 \pm \frac{0.99}{1.10}$
−50	1.62 ± 0.1	$-10.34 \pm \frac{2.04}{2.46}$	$-3.61 \pm \frac{0.71}{0.85}$	$-9.23 \pm \frac{1.00}{1.12}$
−40	1.46 ± 0.1	$-10.80 \pm \frac{2.10}{2.60}$	$-3.75 \pm \frac{0.73}{0.90}$	$-8.88 \pm \frac{0.98}{1.10}$
Weighted average		−10.71 ± 1.03	−3.72 ± 0.36	−8.97 ± 0.45

well extends farther into the plasma. The average height measurements for 10 stably levitated polystyrene grains are listed in Table 2. The error in the height measurement is experimental uncertainty. The corresponding dust potential, dust charge, and electric field at each levitation height from equation (9) are also listed in Table 2. The errors on dust potential and charge are due to both the measured height uncertainty and the range of particle sizes.

[27] It is expected that a grain will levitate at a different height within the sheath depending on the surface bias but will obtain approximately the same potential. Therefore the average potential and charge on a dust grain are calculated using weighted errors. Within the errors, the average dust potentials for each surface bias are constant. These data are shown in Figure 5b. For the five different surface voltages tested, the experimental weighted averaged dust potential and charge on a 10.0 (±0.5) μm polystyrene grain are $\varphi_d = -10.71$ (±1.03) V and $Q_d = -3.72$ (±0.36) × $10^4 e$.

[28] The potential on each grain is also calculated using the OML model presented in section 2. The potential and charge corresponding to each of the measured levitation heights at each of the surface biases are listed in Table 3. Again, the error bars are due to the errors in the height measurement and the particle size variation. The weighted average model dust potential and charge on a 10.0 (±0.5) μm polystyrene grain are $\varphi_{d\mathrm{OML}} = -12.16$ (±0.66) V and $Q_{d\mathrm{OML}} = -4.23$ (±0.23) × $10^4 e$. The average theoretical potentials are compared to the experimental averages in Figure 5b. Using the measured levitation heights, there is good agreement between the dust potentials calculated using equation (9) and those from the OML model.

[29] We can also determine the height at which the particles levitate in stable equilibrium by using OML theory along with the balance of forces. The dust potential calculated by the model, $\varphi_{d\mathrm{OML}}(z)$, and the dust potential calculated by solving the force balance equation, $\varphi_d(z)$, are plotted in Figure 6. There are two different particle levitation heights at which these dust potentials are equal. In order to determine which of these equilibrium points is the stable levitation height, the forces acting on the dust particle are examined. Figure 7a shows each of the forces $F_e(z)$ and F_g as functions of distance from the surface for $V_b = -40$ V. The forces balance at two equilibrium points, labeled z_1 and z_2. The total mechanical potential, as defined in equation (12), is plotted as a function of distance from the surface in Figure 7b. From this plot, it is apparent that z_1 is an unstable equilibrium point, while z_2 is a stable equilibrium point. A grain resting in z_1 will either fall to the surface or be forced upward by the electric field if it is slightly perturbed. On the other hand, a grain slightly displaced from z_2 will be forced back into the equilibrium position. Therefore the point of intersection of dust potentials $\varphi_{d\mathrm{OML}}(z)$ and $\varphi_d(z)$ that is farthest from the surface is the stable equilibrium point. This is the height at which the dust should levitate in order for the OML model of dust potential to match the dust potential obtained by balancing forces. Employing this method for each surface bias, the calculated levitation heights for a 10.0 (± 0.5) μm polystyrene grain are listed in Table 3. These calculated heights as a function of surface bias are shown along with the measured heights in Figure 5a.

[30] The agreement between the experimental levitation heights and the calculated levitation heights is within the error bars. However, the model heights are consistently slightly higher than the measured levitation heights. There are a few possible reasons for this shift. First, the observed dust particles could be biased toward the largest grains in the sample (closer to 10.5 μm than 10.0 μm) and thus levitate lower. Second, there may be inconsistencies between the OML model and the experiment. For example, the model ion current to the surface is assumed by continuity to be constant. However, the ion current to the surface as a function of surface bias has been measured and varies significantly (by a factor of a few). A more

Table 3. OML Model Results for Levitated Polystyrene Grains in the Plasma Sheath

Surface Bias, V_b, V	Potential at Measured Height, $\varphi_{d\mathrm{OML}}$, V	Charge at Measured Height, $Q_{d\mathrm{OML}}$ ($10^4 e$)	Calculated Levitation Height, cm
−80	$-12.14 \pm \frac{1.54}{1.43}$	$-4.21 \pm \frac{0.53}{0.50}$	$2.29 \pm \frac{0.19}{0.33}$
−70	$-12.00 \pm \frac{1.51}{1.43}$	$-4.21 \pm \frac{0.52}{0.50}$	$2.15 \pm \frac{0.19}{0.30}$
−60	$-11.97 \pm \frac{1.57}{1.43}$	$-4.15 \pm \frac{0.54}{0.50}$	$2.01 \pm \frac{0.18}{0.27}$
−50	$-12.22 \pm \frac{1.56}{1.40}$	$-4.24 \pm \frac{0.54}{0.49}$	$1.82 \pm \frac{0.17}{0.23}$
−40	$-12.44 \pm \frac{1.51}{1.41}$	$-4.32 \pm \frac{0.52}{0.49}$	$1.63 \pm \frac{0.17}{0.23}$
Weighted average	−12.16 ± 0.66	−4.23 ± 0.23	

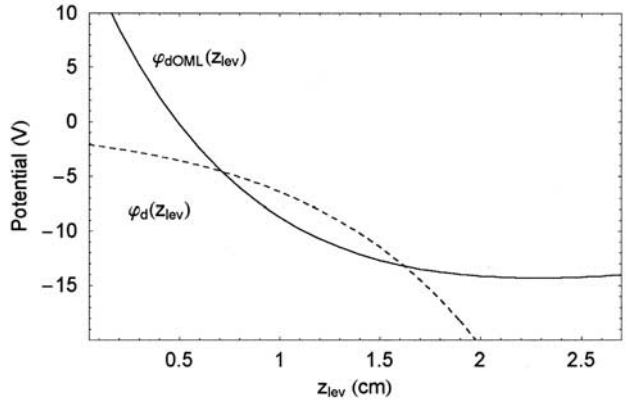

Figure 6. The dust potential, $\varphi_d(z)$, calculated from equation (9) and plotted as a dashed line, and the dust potential, $\varphi_{d\mathrm{OML}}(z)$, shown as a solid line and calculated from equation (2) as functions of dust levitation height, z_{lev}. The two points of intersection are heights at which a dust particle must levitate in order for the dust potentials to be equal.

accurate accounting of the currents to a dust grain in the sheath would greatly aid the model. The inaccuracies in the charging current model can also account for the slight offset in the dust potentials calculated using the measured levitation heights (Figure 5b).

3.3.2. Levitation of Polystyrene Microspheres With UV

[31] The photoemission current from planetary bodies exposed to sunlight is typically significantly larger than the currents of electrons and ions from the solar wind. In this case, a photoelectron sheath is created above the surface and the body becomes positively charged. Positively charged dust particles can then levitate in the photoelectron sheath [e.g., *Gold*, 1955; *Criswell*, 1972; *Nitter et al.*, 1998]. In the experiment presented here, the intensity of the UV light is weak enough that the plasma electron and ion currents to the surface are much larger than photoemission. Thus the experiment remains more like the dark side of a planetary body, with a surface having plasma sheath. The UV primarily affects only the charge on dust particles within the sheath.

[32] Levitation heights of polystyrene microspheres that were exposed to light from the UV source were measured. The observed heights and the corresponding dust potentials and charges calculated by balancing the forces are listed in Table 4 for each surface bias. These observations show that grains consistently levitate at a slightly lower height, and thus a slightly less negative potential, when exposed to UV. Consequently, the average electric field at which dust particles levitate is slightly larger than that required for levitation without UV: −10.24 (±0.51) V/cm versus −8.97 (±0.45) V/cm. For the five different surface voltages tested, the experimental weighted average dust potential and charge on a 10.0 (±0.5) μm polystyrene microsphere are $\varphi_{d\mathrm{UV}} = -9.41$ (±0.89) V and $Q_{d\mathrm{UV}} = -3.26$ (±0.23) × $10^4 e$.

[33] There are two methods by which UV can alter levitation height. First, if UV causes photoemission from the plate surface, then the potential profile in the sheath can be altered. However, measurements of photoemission from various types of surfaces (stainless steel, zirconium, and zinc) indicate that the photocurrent is at least three orders of magnitude less than the current generated by the plasma. In addition, emissive probe measurements did not detect a significant alteration of the sheath profile when the surface was exposed to UV. Therefore photoemission from the surface is negligible.

[34] A second way that UV can alter levitation height is if the grains themselves photoemit. In this case, the grain charge is more positive than that expected merely from collection of ions and electrons from the plasma. Since grains in the sheath are negatively charged, becoming more positive would decrease the charge and grains would levitate closer to the surface where the electric field is larger. The photoelectric work function of polystyrene is not well known. We can obtain an estimate of the work function required for the UV exposed dust to levitate at the observed height by calculating the photoemission current. The current from a particle due to photoemission is given by

$$I_{ph} = \frac{A}{4} n_{ph} e \varepsilon, \tag{15}$$

where n_{ph} is the flux of incoming photons and ε is the photoemission efficiency of the particle. Equation (2) is

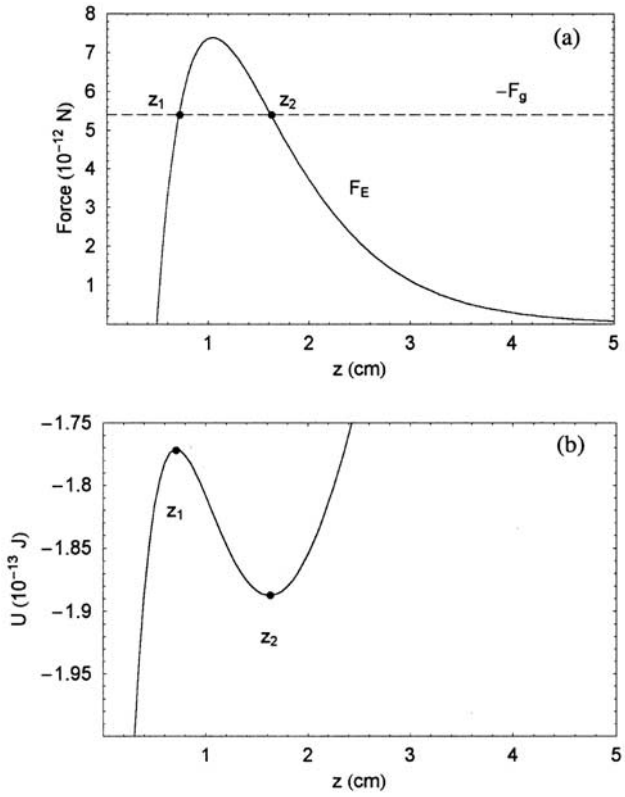

Figure 7. (a) Forces on a dust grain in the sheath as a function of distance from the surface, z. The solid line is the electric force on a particle calculated from equation (10) and using the dust potential $\varphi_{d\mathrm{OML}}(z)$. The dotted line is the negative of the gravitational force on a 10.0 μm polystyrene particle from equation (11). The equilibrium levitation points, where the forces balance, are labeled as z_1 and z_2. (b) The potential energy, $U(z)$, as a function of distance from the surface calculated from equation (12). This plot shows that equilibrium point z_1 is unstable, while z_2 is stable. For each of these plots, the surface is biased to −40 V.

Table 4. Data for Levitated Polystyrene Grains in Plasma Sheath Exposed to UV Source

Surface Bias, V_b, V	Measured Levitation Height, cm	Potential at Measured Height, $\varphi_{d\mathrm{UV}}$, V	Charge at Measured Height, $Q_{d\mathrm{UV}}$ (10^4 e)	Electric Field at Measured Height, E, V/cm
−80	2.08 ± 0.1	$-10.02 \pm ^{1.88}_{2.25}$	$-3.48 \pm ^{0.65}_{0.78}$	$-9.63 \pm ^{0.96}_{1.07}$
−70	1.87 ± 0.1	$-9.50 \pm ^{1.82}_{2.18}$	$-3.30 \pm ^{0.63}_{0.75}$	$-10.20 \pm ^{1.06}_{1.18}$
−60	1.69 ± 0.1	$-9.13 \pm ^{1.76}_{2.12}$	$-3.17 \pm ^{0.61}_{0.73}$	$-10.59 \pm ^{1.11}_{1.25}$
−50	1.51 ± 0.1	$-9.22 \pm ^{1.18}_{2.18}$	$-3.20 \pm ^{0.63}_{0.76}$	$-10.47 \pm ^{1.14}_{1.28}$
−40	1.31 ± 0.1	$-9.20 \pm ^{1.81}_{2.19}$	$-3.19 \pm ^{0.63}_{0.76}$	$-10.57 \pm ^{1.16}_{1.31}$
Weighted average		−9.41 ± 0.89	−3.26 ± 0.23	−10.24 ± 0.51

then combined with equation (15) to obtain a new current balance equation,

$$I_e(z) + I_i(z) + I_{ph} = 0. \tag{16}$$

We calculate n_{ph} from the properties of the light source and the work function of the dust, and we measure the height of a levitating particle exposed to UV. For the plate bias V_b = −40 V, a 10.0 μm polystyrene particle is observed to levitate at 1.31 (±0.1) cm (see Table 4). Typical photoemission efficiencies are $\varepsilon \approx 1$ for metals and $\varepsilon \approx 0.1$ for dielectrics [*Goertz*, 1989]. Assuming z = 1.31 cm and ε = 0.1, equation (16) is solved when the work function of the particle is 5.12 eV. This value can be compared to the experimental work function derived for silica particles resting on a surface, 5.5 eV [*Sternovsky et al.*, 2001].

[35] These results suggest that levitation heights of dust grains are slightly affected by UV, even if the particles have large work functions or low photoefficiency. For grains on planetary surfaces, this may lead to dust being levitated or dropped onto the surface depending on rotation into or out of sunlight.

3.3.3. Levitation of Glass Microballoons and JSC-1

[36] In addition to standard-sized polystyrene microspheres, two other types of levitated dust are used. Hollow glass microballoons <38 μm in diameter were the first type of particles levitated in the chamber due to their large charge to mass ratio. These particles levitate at heights of approximately 1–2 cm above the surface when the surface is biased to −40 V. The mass of these particles is uncertain because of the range in particle diameter and the variation in wall thickness. By balancing the forces, we can determine that the particles observed to levitate at these heights should be approximately 6–22 μm in diameter.

[37] In order to determine the likelihood of dust levitation above surfaces in space, we performed experiments on JSC-1, a lunar regolith simulant. The smallest particle size available from sieving is <25 μm in diameter. When the surface is biased to −50 V, JSC-1 grains of this size range are observed to levitate approximately 0.8–2.0 cm above the surface. The grain sizes required for the forces to balance at these heights are approximately 2–10 μm in diameter. This size range is on the same order as the particles thought to cause the observed lunar horizon glow [*Rennilson and Criswell*, 1974]. Larger particle sizes can be levitated when the surface is biased more negatively. In addition, when multiple particles are levitated simultaneously, the dynamics become quite complicated. Owing to dust-dust interactions, particles move both horizontally and vertically above the surface.

[38] One of the difficulties with obtaining dust levitation is having sufficient force to overcome surface adhesion. Although the experiment has an agitator, which hits the surface and injects dust particles into the plasma sheath, this mechanism is not necessary. All types of dust particles are launched into the sheath without agitation when the surface bias is less than approximately −30 V. The larger the surface bias, the larger the number of particles observed lifting upward from the surface.

[39] These results suggest that it is fairly easy to levitate and move many kinds of dust particles above a surface with a plasma sheath. In space, the probability for levitation depends on ambient plasma properties and the sizes of particles resting on the surface. Dust levitation above the moon and asteroids has been considered primarily in terms of particles within photoelectron sheaths [e.g., *Pelizzari and Criswell*, 1978; *Lee*, 1996], because surface charge density and electric fields are very high under sunlight. However, our experiments suggest that dust levitation in plasma sheaths in space may also occur. Surfaces in space are covered with particles of very small sizes, and there are micrometeoroid impacts that eject them from the surface. In addition, the electric field at the lunar terminator can be 500–1500 V/cm [*Rennilson and Criswell*, 1974]. For comparison, the electric field on a surface biased to −40 V in the experiment is −48.6 V/cm.

[40] In order to determine whether the electric force generated by this field should be large enough to launch particles from the surface, the surface adhesion force needs to be considered. A particle resting on the surface will feel the electric force acting upward and gravity and an adhesion force acting downward. In the experiment, particles do not release from the surface when it is biased to −30 V, but they are released when V_b = −40 V. We can solve for the adhesion force, F_a, using the force balance equation

$$F_e(z) - F_g - F_a = 0, \tag{17}$$

for z = 0 cm and V_b = −30 V. Assuming a particle on the surface reaches the same potential as the surface, the adhesion force is 5.7×10^{-11} N. Lunar regolith may have higher adhesive forces depending on the size distribution and shape of the grains [*Lee*, 1995]. On Earth, the adhesive force is ten times the gravitational force on a 10.0 μm polystyrene particle. On the Moon or on an asteroid, the adhesive force would be even larger relative to gravity. When a surface is biased negatively enough to overcome the adhesion force, particles are launched upward. After the particle breaks free from the surface, its charge adjusts to the near-surface plasma

current, and it accelerates upward. Depending on the relative strength of the gravitational acceleration, the upward electric force, and the particle's initial acceleration from the surface, a dust grain may reach escape velocity, be stably levitated as we have demonstrated here, or return to the surface.

[41] The surface in the experiments presented here is externally biased to compensate for the large gravity on Earth. Surfaces in space can also reach large potentials due to charging currents in the plasma and the low conductivity of rocks and soil. Models of the potential on the nightside of the Moon suggest that it can be very large, reaching up to −1800 V [*Manka*, 1973; *Mall and Borisov*, 2001]. This is due to the fact that the solar wind plasma temperature is ≈10 eV and the velocity is ≈400 km/s, so that electrons are subsonic while ions are supersonic. More recently, measurements from Lunar Prospector imply a nighttime lunar surface potential of −35 to −230 V [*Halekas et al.*, 2002]. The potential on the dark hemisphere of a comet at 5 AU can be −550 to −2550 V, depending on solar wind and surface conditions [*Mendis et al.*, 1981]. These surface potentials are significantly larger, and the gravity significantly lower, than those required for dust levitation in the experiments presented here.

4. Conclusions

[42] We have conducted experiments on the levitation of dust particles in an argon plasma sheath above a biased surface. Levitated particles include polystyrene microspheres, glass microballoons, and JSC-1 lunar regolith simulant. Dust particles are observed to levitate singly or in clouds. Observations are made of single, levitated polystyrene grains (chosen for their well-defined mass). The dust potential and charge of a levitated grain calculated using OML theory agrees well with those deduced from balancing the forces in the sheath, given the measured levitation height. The levitation height as a function of surface bias, obtained by selecting the stable intersection of the dust potential from OML theory with the dust potential from force balance, also agrees well with the measured height.

[43] Particles exposed to a UV source consistently levitate at a slightly lower height than particles not exposed to UV light. This is most likely due to photoemission from the particles, which causes the dust potential to be less negative. Exposure to UV light may cause particles to drop out of the sheath and be deposited onto the surface. Particles are not always stationary within the sheath; they are observed to move both vertically and horizontally above the surface. Thus UV exposure may result in dust falling out of the sheath in a different location than it entered. This is one mechanism by which dust can be transported across a surface.

[44] These experiments support the model of electrostatic processes being the primary cause of dust levitation and transport near surfaces in space. Many different types of particles levitate under a variety of plasma environments. In addition, conditions that are even more conducive to dust levitation than those in the experiments are found throughout the solar system.

[45] Future experiments include a more detailed investigation of JSC-1 levitation and motion above a surface having a plasma sheath. In particular, we plan to study the horizontal transport of dust particles above surfaces of different compositions and having varied topography. These experiments can be compared to observations of dust dynamics above the Moon and those that might have occurred on the surface of Eros.

[46] **Acknowledgments.** The authors acknowledge support from NASA (NAG3-2136 and NGT5-50294). We also thank Zoltán Sternovsky for his assistance.

[47] Shadia Rifai Habbal thanks Wing-Huen Ip and D. Asoka Mendis for their assistance in evaluating this paper.

References

Arnas, C., M. Mikikian, and F. Doveil, High negative charge of dust particles in a hot cathode discharge, *Phys. Rev. E*, *60*(6), 7420–7425, 1999.

Arnas, C., M. Mikikian, G. Bachet, and F. Doveil, Sheath modification in the presence of dust particles, *Phys.Plasmas*, *7*(11), 4418–4422, 2000.

Arnas, C., M. Mikikian, and F. Doveil, Micro-sphere levitation in a sheath of a low pressure continuous discharge, *Phys. Scr. T*, *89*, 163–167, 2001.

Bernstein, I. B., and I. N. Rabinowitz, Theory of electrostatic probes in low-density plasma, *Phys. Fluids*, *2*, 112–121, 1959.

Bohm, D., Minimum ionic kinetic energy for a stable sheath, in *The Characteristics of Electrical Discharges in Magnetic Fields*, edited by A. Guthrie and R. K. Wakerling, p. 77, McGraw-Hill, New York, 1949.

Criswell, D. R., Lunar dust motion, Proc, *Lunar Planet. Sci. Conf.*, *3rd*, 2671–2680, 1972.

Diebold, D., N. Hershkowitz, A. D. Bailey III, M. H. Cho, and T. Intrator, Emissive probe current bias method of measuring dc vacuum potential, *Rev. Sci. Instrum.*, *59*(2), 270–275, 1988.

Doe, S. J., O. Burns, D. Pettit, J. Blacic, and P. W. Keaton, The levitation of lunar dust via electrostatic forces, in *Engineering, Construction, and Operations in Space*, pp. 907–915, Am. Soc. of Civ. Eng., Reston, Va., 1994.

Goertz, C. K., Dusty plasmas in the solar system, *Rev. Geophys.*, *27*(2), 271–292, 1989.

Gold, T., The lunar surface, *Mon. Not.R. Astron. Soc.*, *115*, 585–604, 1955.

Halekas, J. S., D. L. Mitchell, R. P. Lin, L. L. Hood, M. H. Acuña, and A. B. Binder, Evidence for negative charging of the lunar surface in shadow, *Geophys. Res. Lett.*, *29*(10), 1435, 10.1029/2001GL014428, 2002.

Ip, W. H., Electrostatic charging and dust transport at Mercury's surface, *Geophys. Res. Lett.*, *13*, 1133–1136, 1986.

Lee, L. H., Adhesion and cohesion mechanisms of lunar dust on the Moon's surfaces, *J. Adhesion Sci. Technol.*, *9*(8), 1103–1124, 1995.

Lee, P., Dust levitation on asteroids, *Icarus*, *124*, 181–194, 1996.

Lieberman, M. A., and A. J. Lichtenberg, *Principles of Plasma Discharge and Materials Processing*, John Wiley, New York, 1994.

Mall, U., and N. Borisov, Electric potential distribution on the nightside of the Moon, *Lunar Planet. Sci.*, [CD-ROM], XXXII, abstract 1538 2001.

Manka, R. H., Lunar ion energy spectra and surface potential, *Proc. Lunar Planet. Sci. Conf, 4th*, 496–497, 1973.

McKay, D. S., J. L. Carter, W. W. Boles, C. C. Allen, and J. H. Alton, JSC-1: A new lunar soil simulant, in *Engineering, Construction, and Operations in Space IV*, pp. 857–866, Am. Soc. of Civ. Eng., Reston, Va., 1994.

Mendis, D. A., J. R. Hill, H. L. F. Houpis, and E. C. Whipple, Jr., On the electrostatic charging of the cometary nucleus, *Astrophys. J.*, *249*, 787–797, 1981.

Nitter, T., O. Havnes, and F. Melandsø, Levitation and dynamics of charged dust in the photoelectron sheath above surfaces in space, *J. Geophys. Res.*, *103*, 6605–6620, 1998.

Pelizzari, M. A., and D. R. Criswell, Lunar dust transport by photoelectric charging at sunset, *Proc. Lunar Planet. Sci. Conf.*, *9th*, 3225–3237, 1978.

Rennilson, J. J., and D. R. Criswell, Surveyor observations of lunar horizon glow, *Moon*, *10*, 121–142, 1974.

Robinson, M. S., P. C. Thomas, J. Veverka, S. Murchie, and B. Carcich, The nature of ponded deposits on Eros, *Nature*, *413*, 396–400, 2001.

Samsonov, D., A. V. Ivelev, G. E. Morfill, and J. Goree, Long-range attractive and repulsive forces in a two-dimensional complex (dusty) plasma (on line), *Phys. Rev.E.*, *63*(2), id 025401 2001.

Sickafoose, A. A., J. E. Colwell, M. Horányi, and S. Robertson, Photoelectric charging of dust particles in vacuum, *Phys. Rev. Lett.*, *84*, 6034–6037, 2000.

Sickafoose, A. A., J. E. Colwell, M. Horányi, and S. Robertson, Experimental investigations on photoelectric and triboelectric charging of dust, *J. Geophys. Res.*, *106*, 8343–8356, 2001.

Singer, S. F., and E. H. Walker, Electrostatic dust transport on the lunar surface, *Icarus*, *1*, 112–120, 1962.

Sternovsky, Z., M. Horányi, and S. Robertson, Charging of dust particles on surfaces, *J. Vac. Sci. Technol. A.*, *19*(5), 2533–2541, 2001.

Veverka, J., Imaging of small-scale features on 433 Eros from NEAR: Evidence for a complex regolith, *Science*, *292*, 484–488, 2001.

Walch, B., M. Horányi, and S. Robertson, Charging of dust grains in plasma with energetic electrons, *Phys. Rev. Lett.*, *75*, 838–841, 1995.

Zook, H. A., and J. E. McCoy, Large-scale lunar horizon glow and a high altitude lunar dust exosphere, *Geophys. Res. Lett.*, *18*, 2117–2120, 1991.

Zook, H. A., A. E. Potter, and B. L. Cooper, The lunar dust exosphere and Clementine lunar horizon glow, *Lunar Planet. Sci.*, *26*, 1577–1578, 1995.

J. E. Colwell and A. A. Sickafoose, Laboratory for Atmospheric and Space Physics, University of Colorado, Campus Box 392, Boulder, Colorado 80309-0392, USA. (amanda@casper.colorado.edu; colwell@casper.colorado.edu)

M. Horányi and S. Robertson, Department of Physics, University of Colorado, Boulder, Colorado 80309, USA. (mihaly.horanyi@lasp.colorado.edu; robertso@stripe.colorado.edu)